Recoverability geometry: distances and embeddings from quantum Markov data

Definitions, diagnostics, and a reconstruction protocol

Lluis Eriksson
Independent Researcher
lluiseriksson@gmail.com

January 2026

Abstract

We propose an operational route from recoverability data to effective geometry. Given a tripartition A–$B(w)$–C and a collar width w, we consider a Petz-type recoverability error $E_{\mathrm{rec}}^{\mathrm{Petz}}(w)$ defined via fidelity and extracted from a fixed collaring rule $(A, C, w) \mapsto B_{A,C}(w)$. We then define distance-like functionals from the minimal buffer needed to suppress $E_{\mathrm{rec}}^{\mathrm{Petz}}(w)$ below a threshold, and from exponential fit scales when such a regime exists. These can be organized into a (generally non-metric) dissimilarity matrix on coarse regions, symmetrized when needed, and embedded into low-dimensional spaces using multidimensional scaling or diffusion maps. The paper emphasizes precise definitions (collaring rule, symmetrization, censoring below numerical floors) and falsifiable diagnostics (approximate triangle inequalities, robustness to thresholds and regularization). A minimal control experiment in the one-dimensional transverse-field Ising model illustrates the pipeline and the growth of a recoverability length near criticality.

Contents

1 Introduction **3**

2 Preliminaries: fidelity and Petz-type recovery **3**
2.1 Fidelity and recovery error . . . 3
2.2 Tripartitions and collar width . . . 3
2.3 Regularized Petz-type map and normalization convention . . . 3

3 The collaring rule as part of the input **4**

4 From recoverability profiles to distance-like objects **4**
4.1 Directed and symmetrized threshold distances . . . 4
4.2 A more robust (persistent) threshold . . . 5
4.3 Exponential-fit scale . . . 5

5 Affinities, kernels, and embeddings **5**
5.1 A symmetric affinity kernel . . . 5
5.2 Embedding recipes . . . 5

6 Geometric diagnostics (desiderata rather than hypotheses) **6**

7 Minimal numerical illustration: TFIM control **6**
7.1 Model . . . 6
7.2 Representative fit data . . . 6

8 Conjectures and model comparisons **8**

9 Protocol summary **8**

10 Discussion and outlook **8**

1 Introduction

The idea that geometry may be inferred from quantum-information patterns appears in several guises: entanglement entropy and minimal surfaces in AdS/CFT [4], tensor-network constructions such as MERA [5], and quantum error-correcting code toy models for bulk reconstruction [6]. This work focuses on a different input: *recoverability*.

Given a state on ABC, recoverability asks whether the state on BC can be approximately reconstructed from the state on B alone, using a recovery map acting only on B. Small recovery error indicates approximate quantum Markov structure. The main proposal of this note is to treat the *buffer width needed* to achieve small recovery error as a proxy for an *effective distance* between A and C, and to use these effective distances to build embeddings that can be compared to underlying lattice geometry and to physical length scales (correlation length, confinement scale, ...).

Scope and non-claims. We do not claim a unique emergent manifold or a theorem-level continuum limit. The output is a family of operationally defined distance-like objects that can succeed (approximate metric behavior) or fail (useful diagnostics of non-geometric regimes).

2 Preliminaries: fidelity and Petz-type recovery

2.1 Fidelity and recovery error

For density matrices ρ and σ on a finite-dimensional Hilbert space, we use the squared Uhlmann fidelity

$$F(\rho,\sigma) := \left(\mathrm{Tr}\sqrt{\sqrt{\rho}\,\sigma\,\sqrt{\rho}}\right)^2 \in [0,1],$$

and define the recovery error

$$E_{\mathrm{rec}}(\rho \to \sigma) := -\log F(\rho,\sigma).$$

2.2 Tripartitions and collar width

Let $\mathcal{L}$ be a finite graph (e.g. a lattice). Fix disjoint regions $A, C \subset \mathcal{L}$ and a family of buffer regions $B(w)$ indexed by a collar width $w \in \mathbb{N}$. Unless stated otherwise, widths are measured in graph-distance units at fixed lattice spacing.

2.3 Regularized Petz-type map and normalization convention

Let ρ_{ABC} be a density matrix on $\mathcal{H}_A \otimes \mathcal{H}_B \otimes \mathcal{H}_C$, and write $\rho_B = \mathrm{Tr}_{AC}(\rho_{ABC})$ and $\rho_{BC} = \mathrm{Tr}_A(\rho_{ABC})$. Fix $\delta > 0$ and define $\rho_{B,\delta} := \rho_B + \delta\,\mathbf{1}_B$.

Definition 2.1 (Regularized Petz-type map)**.** Define $\mathcal{R}^{\mathrm{Petz}(\delta)}_{B\to BC}$ by

$$\mathcal{R}^{\mathrm{Petz}(\delta)}_{B\to BC}(X_B) := \rho_{BC}^{1/2}\left(\rho_{B,\delta}^{-1/2}\, X_B\, \rho_{B,\delta}^{-1/2} \otimes \mathbf{1}_C\right)\rho_{BC}^{1/2}.$$

Remark 2.2 (Normalization). For $\delta > 0$, $\mathcal{R}^{\mathrm{Petz}(\delta)}$ is completely positive but not necessarily trace-preserving. In numerical implementations we therefore normalize reconstructed outputs by their trace before computing fidelity.

Definition 2.3 (Recoverability profile)**.** For a family of tripartitions $(A, B(w), C)$, define the (possibly unnormalized) reconstructed operator

$$\widetilde{\rho}_{ABC}(w) := (\mathrm{id}_A \otimes \mathcal{R}^{\mathrm{Petz}(\delta)}_{B\to BC})(\rho_{AB}),$$

and the normalized state $\widehat{\rho}_{ABC}(w) := \widetilde{\rho}_{ABC}(w)/\mathrm{Tr}(\widetilde{\rho}_{ABC}(w))$ whenever the trace is positive. Define

$$E^{\mathrm{Petz}}_{\mathrm{rec}}(A \to C; w) := -\log F\Big(\rho_{ABC},\, \widehat{\rho}_{ABC}(w)\Big).$$

3 The collaring rule as part of the input

A recoverability distance is not well-defined unless the growth rule for the buffer is fixed.

Definition 3.1 (Collaring rule)**.** A *collaring rule* is a deterministic assignment which, for each ordered pair of disjoint regions (A, C) in $\mathcal{L}$ and each $w \in \mathbb{N}$, produces a region $B_{A,C}(w) \subset \mathcal{L}$ such that:

1. A, $B_{A,C}(w)$, and C are pairwise disjoint,
2. $B_{A,C}(w) \subseteq B_{A,C}(w+1)$ (nested buffers),
3. $B_{A,C}(w)$ is intended to "separate" A from C (model-dependent; e.g. every path from A to C intersects $B_{A,C}(w)$ once w exceeds a minimal separating width).

All profiles $E^{\mathrm{Petz}}_{\mathrm{rec}}(A \to C; w)$ and derived distances in this paper are understood *relative to a fixed choice* of collaring rule.

Remark 3.2 (Canonical choices). On regular lattices with planar or rectangular region families, a common choice is to thicken a fixed separating cut surface by graph distance w. In one-dimensional chains with contiguous blocks, $B_{A,C}(w)$ is naturally taken as the w-site buffer between A and C. Different collaring rules define different recoverability distances; comparing them is itself a diagnostic.

4 From recoverability profiles to distance-like objects

4.1 Directed and symmetrized threshold distances

Definition 4.1 (Directed threshold recoverability distance)**.** Fix $\varepsilon > 0$ and a collaring rule $B_{A,C}(w)$. Define

$$d^{(\varepsilon)}_{\mathrm{rec}}(A \to C) := \min\{\, w :\ E^{\mathrm{Petz}}_{\mathrm{rec}}(A \to C; w) \le \varepsilon \,\},$$

whenever the set is nonempty.

Remark 4.2. The arrow reminds us that the construction can be convention-dependent and effectively directional (depending on how $B_{A,C}(w)$ is defined and how reconstruction is implemented). In many symmetric settings one expects $d^{(\varepsilon)}_{\mathrm{rec}}(A \to C) \approx d^{(\varepsilon)}_{\mathrm{rec}}(C \to A)$, but we do not assume this.

Definition 4.3 (Symmetrized recoverability distance)**.** When both directed distances are defined, set

$$d^{(\varepsilon)}_{\mathrm{rec,sym}}(A, C) := \max\{d^{(\varepsilon)}_{\mathrm{rec}}(A \to C),\, d^{(\varepsilon)}_{\mathrm{rec}}(C \to A)\}.$$

If one direction is undefined, $d^{(\varepsilon)}_{\mathrm{rec,sym}}(A, C)$ is treated as undefined (or capped at a chosen maximum in numerical work).

4.2 A more robust (persistent) threshold

Finite-size and numerical noise can produce small non-monotone fluctuations in $E^{\mathrm{Petz}}_{\mathrm{rec}}(w)$. A robust alternative is to require the threshold to hold persistently beyond w.

Definition 4.4 (Persistent threshold distance)**.** Fix $\varepsilon > 0$ and a maximum computed collar width $w_{\max} \in \mathbb{N}$. Define

$$d^{(\varepsilon)}_{\mathrm{rec,pers}}(A \to C) := \min\Big\{ w \in \{1, \dots, w_{\max}\} : \max_{w' \in \{w, w+1, \dots, w_{\max}\}} E^{\mathrm{Petz}}_{\mathrm{rec}}(A \to C; w') \le \varepsilon \Big\},$$

whenever the set is nonempty.

4.3 Exponential-fit scale

Definition 4.5 (Recoverability length scale)**.** If $E^{\mathrm{Petz}}_{\mathrm{rec}}(w)$ exhibits an approximate exponential window on $w \in [w_{\min}, w_{\max}]$, define ξ_{rec} by the slope of a linear fit

$$\log E^{\mathrm{Petz}}_{\mathrm{rec}}(w) \approx \log A - \frac{w}{\xi_{\mathrm{rec}}}.$$

Remark 4.6 (Numerical floors and censoring). When $E^{\mathrm{Petz}}_{\mathrm{rec}}(w)$ falls below a numerical floor (e.g. $E^{\mathrm{Petz}}_{\mathrm{rec}}(w) \le 10^{-14}$ in double precision), semilog fits become unreliable. Fits should be performed only on points with $E^{\mathrm{Petz}}_{\mathrm{rec}}(w)$ above a chosen floor and within a stable fit window; otherwise ξ_{rec} should not be reported.

5 Affinities, kernels, and embeddings

5.1 A symmetric affinity kernel

Definition 5.1 (Recoverability affinity kernel)**.** Fix $\alpha > 0$ and $\varepsilon > 0$. Define a symmetric dissimilarity between coarse regions A_i, A_j by

$$D_{ij} := d^{(\varepsilon)}_{\mathrm{rec,sym}}(A_i, A_j),$$

with a chosen convention for undefined entries (e.g. treat as missing data, or cap at a maximum value). Define the kernel

$$K_{ij} := \exp(-\alpha D_{ij}),$$

and set $K_{ii} := 1$.

Remark 5.2 (Missing data). If many D_{ij} are undefined, kernel methods are typically applied on a neighborhood graph (e.g. k-nearest neighbors with respect to defined D_{ij}) or on the largest connected component induced by nonzero affinities. In our numerical illustrations we treat undefined entries as missing and build a k-nearest-neighbor graph on the defined distances before applying diffusion maps.

5.2 Embedding recipes

Two standard routes are:

- *Classical multidimensional scaling (MDS)* applied to D_{ij} (when D is approximately metric).
- *Diffusion maps* applied to K_{ij} (often more robust under noise and missing entries) [7].

We treat the embedding as a diagnostic summary rather than a unique geometric reconstruction.

6 Geometric diagnostics (desiderata rather than hypotheses)

We now state properties one can *test* in data; these are not assumptions about Nature, but desirable consistency checks indicating when recoverability behaves geometrically.

Criterion 6.1 (Effective monotonicity)**.** For fixed A and C, the profile $E_{\mathrm{rec}}^{\mathrm{Petz}}(w)$ is approximately non-increasing in w over the range used for thresholding and fits.

Criterion 6.2 (Robustness to thresholds and regularization)**.** There exist intervals $\varepsilon \in [\varepsilon_-, \varepsilon_+]$ and $\delta \in [\delta_-, \delta_+]$ such that extracted distances and embeddings are stable (up to bounded distortions) under these variations.

Definition 6.3 (Triangle-violation score)**.** Given three coarse regions A_i, A_j, A_k, define

$$\Delta_{ijk} := \max\{0,\ D_{ik} - D_{ij} - D_{jk}\},$$

where D_{ab} denotes the symmetrized recoverability distance (when defined).

Large Δ_{ijk} signals either non-geometric behavior (long-range constraints, sector structure, etc.) or an incompatible coarse-graining choice.

7 Minimal numerical illustration: TFIM control

This section provides one concrete, self-contained illustration: a control experiment in the one-dimensional transverse-field Ising model (TFIM). The purpose is to show that (i) the recoverability pipeline is implementable and (ii) extracted scales change qualitatively across gapped and near-critical regimes.

7.1 Model

We consider the TFIM Hamiltonian on L spins with open boundary conditions,

$$H = -J \sum_{i=1}^{L-1} Z_i Z_{i+1} - g \sum_{i=1}^{L} X_i - h \sum_{i=1}^{L} Z_i,$$

where X_i and Z_i are Pauli operators acting on site i. For $g < 1$ and finite L, the symmetric ground state can be cat-like; we therefore include a small longitudinal field $h = 10^{-3}$ in the ordered regime to select a symmetry-broken vacuum.

We use contiguous tripartitions A–$B(w)$–C with $|A|$ and $|C|$ fixed, and trace out the complement as an environment D so that varying w increases only the buffer.

7.2 Representative fit data

For parameters $L = 14$, $|A| = 3$, $|C| = 4$, global regularization $\delta = 10^{-12}$, and semilog fits over $w \in \{2, 3, 4\}$ including only points with $E_{\mathrm{rec}}^{\mathrm{Petz}}(A \to C; w) > 10^{-14}$, a representative run yields the values in Table 1. These values are included only to demonstrate the pipeline and parameter dependence; they should not be over-interpreted as universal constants.

g	h	fitted ξ_{rec}	R^2 (semilog fit)
0.5	10^{-3}	1.433	0.6501
1.0	0	4.58	0.9276
2.0	0	0.6515	0.9990

Table 1: TFIM control experiment: recoverability-rate fits on $w \in \{2, 3, 4\}$ for contiguous A–$B(w)$–C with the complement traced out. The ordered regime uses a small symmetry-breaking field $h = 10^{-3}$ to avoid a finite-size cat state.

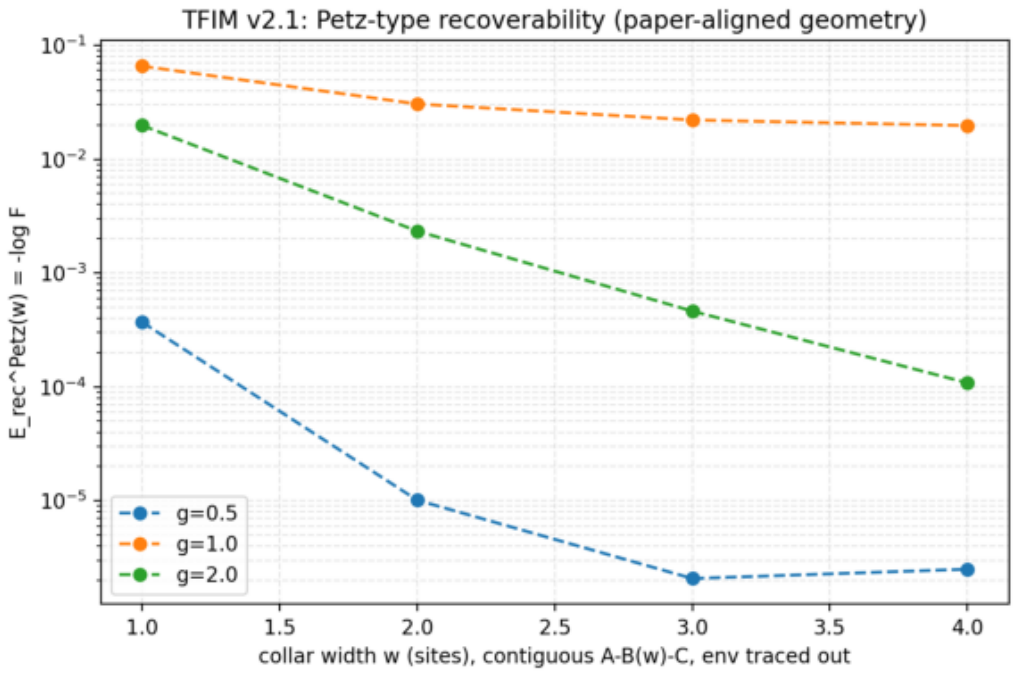

Figure 1: TFIM control experiment. Petz-type recoverability error $E_{\mathrm{rec}}^{\mathrm{Petz}}(w)$ versus collar width w for contiguous tripartitions A–$B(w)$–C with $|A|$ and $|C|$ fixed and the complement traced out. A small longitudinal field $h = 10^{-3}$ is used for $g < 1$ to avoid a finite-size cat state.

Remark 7.1 (What this does and does not show). In one dimension, embedding primarily tests consistency and scale extraction rather than nontrivial manifold reconstruction. The TFIM control illustrates that recoverability scales can be short in deeply gapped regimes and grow near criticality, motivating the use of recoverability-derived distances in more complex settings.

8 Conjectures and model comparisons

Conjecture 8.1 (Recoverability tracks a physical length scale)**.** In gapped phases of local Hamiltonians, for suitable collaring rules and region families, $E_{\mathrm{rec}}^{\mathrm{Petz}}(w)$ admits an exponential window and the extracted ξ_{rec} is finite and of the same order as a conventional correlation length extracted from two-point functions or transfer matrices, up to model- and geometry-dependent constants.

Remark 8.2. This conjecture is falsifiable by explicit computation in solvable models (free fermions, classical transfer matrices) and by numerics in interacting systems. Failures can be physically meaningful, for instance in phases with long-range constraints or strong sector structure.

9 Protocol summary

1. Fix a model, graph $\mathcal{L}$, and state ρ (ground state, thermal state, ...).
2. Fix a subsystem prescription and a collaring rule $B_{A,C}(w)$ for pairs of regions (A, C).
3. Choose coarse regions $\{A_i\}_{i=1}^{N}$ and for each pair compute profiles $E_{\mathrm{rec}}^{\mathrm{Petz}(i,j)}(w)$.
4. Extract directed distances $d_{\mathrm{rec}}^{(\varepsilon)}(A_i \to A_j)$ and symmetrize to D_{ij}.
5. Apply stability checks under ε and δ, and censor below numerical floors.
6. Build affinities $K_{ij} = \exp(-\alpha D_{ij})$ and compute embeddings (MDS, diffusion maps).
7. Diagnose geometric behavior via triangle-violation scores and robustness tests.

10 Discussion and outlook

Recoverability-derived distances provide a concrete, testable bridge between approximate quantum Markov structure and emergent geometry. The central message is operational: define distances from buffer width, symmetrize and censor carefully, and use geometric diagnostics to determine when the resulting objects behave metrically.

Immediate extensions include higher-dimensional spin systems, free-fermion benchmarks with known correlation lengths, and constrained systems (including gauge theories) where subsystem prescriptions introduce additional structure. In the latter case, comparing recoverability-derived distances to confinement diagnostics such as Wilson loops is an important next step.

References

[1] D. Petz, Sufficient subalgebras and the relative entropy of states of a von Neumann algebra, *Communications in Mathematical Physics* **105**, 123–131 (1986).

[2] O. Fawzi and R. Renner, Quantum conditional mutual information and approximate Markov chains, *Communications in Mathematical Physics* **340**, 575–611 (2015).

[3] A. Uhlmann, The "transition probability" in the state space of a $*$-algebra, *Reports on Mathematical Physics* **9**, 273–279 (1976).

[4] S. Ryu and T. Takayanagi, Holographic derivation of entanglement entropy from AdS/CFT, *Physical Review Letters* **96**, 181602 (2006).

[5] B. Swingle, Entanglement renormalization and holography, *Physical Review D* **86**, 065007 (2012).

[6] F. Pastawski, B. Yoshida, D. Harlow, and J. Preskill, Holographic quantum error-correcting codes: toy models for the bulk/boundary correspondence, *Journal of High Energy Physics* **06**, 149 (2015).

[7] R. R. Coifman and S. Lafon, Diffusion maps, *Applied and Computational Harmonic Analysis* **21**, 5–30 (2006).

[8] L. Eriksson, Petz recoverability in AQFT via conditional expectations: a framework and a conditional exponential recovery bound, preprint (2026).

[9] L. Eriksson, Recoverability length scales and Wilson loops in lattice gauge theories: protocol, definitions, and conjectural links to confinement diagnostics, preprint (2026).